



HAL
open science

A robust model-based test planning procedure

Pascal Vinot, Scott Cogan, Valério Cipolla

► **To cite this version:**

Pascal Vinot, Scott Cogan, Valério Cipolla. A robust model-based test planning procedure. *Journal of Sound and Vibration*, 2005, 288 (3), pp.571-585. 10.1016/j.jsv.2005.07.007 . hal-00176856

HAL Id: hal-00176856

<https://hal.science/hal-00176856>

Submitted on 3 May 2023

HAL is a multi-disciplinary open access archive for the deposit and dissemination of scientific research documents, whether they are published or not. The documents may come from teaching and research institutions in France or abroad, or from public or private research centers.

L'archive ouverte pluridisciplinaire **HAL**, est destinée au dépôt et à la diffusion de documents scientifiques de niveau recherche, publiés ou non, émanant des établissements d'enseignement et de recherche français ou étrangers, des laboratoires publics ou privés.



Distributed under a Creative Commons Attribution - NonCommercial 4.0 International License

A robust model-based test planning procedure

P. Vinot^{a,*}, S. Cogan^a, V. Cipolla^b

^aFEMTO-ST Institute, LMARC, 24, rue de l'Épithaphe, 25000 Besançon, France

^bCNES, 18, Avenue Edouard Belin, 31401 Toulouse Cedex 09, France

A wide variety of model-based optimal test design methodologies have been developed in the past decade using deterministic approaches. This means that the test planning is based on a single-nominal model and an optimal design is obtained for precisely this model. Needless to say, the deterministic approach can lead to an ineffective distribution of sensors and poorly defined excitation points due to the presence of epistemic modelling errors. In this article, a robust-satisficing design approach to test planning is proposed based on info-gap decision theory. This methodology provides a decision-making tool for better understanding the trade-off between an optimal test design with no robustness to modelling uncertainties and a sub-optimal design which satisfies a less demanding level of performance while remaining maximally robust with respect to a given horizon of info-gap model uncertainty. The proposed strategy is illustrated using an aerospace application under base excitation conditions.

1. Introduction

Designers are constantly faced with the need to compromise between often antagonistic measures of design success such as: system performance, robustness to uncertainties in the system and its environment, cost of development and manufacturing, cost of system failure, and environmental impact. Expert knowledge combined with model-based decision-making tools can provide a framework for entertaining a greater diversity of candidate solutions by improving the

*Corresponding author. Tel.: +33 3 81 66 60 29; fax: +33 3 81 66 67 00.

E-mail address: pascal.vinot@univ-fcomte.fr (P. Vinot).

Nomenclature

\mathbf{D}_j	j th dof among candidate dof	n	number of dof
\mathbf{F}	$m \times r$ mass modal participation factor matrix	n^s	maximal number of sensors
\mathbf{I}_m	identity matrix of size $m \times m$	r	number of rigid-body modes
\mathbf{L}	sensor location matrix	\mathbf{y}_v^i	v th eigenvector of the i th modal basis
\mathbf{M}_0	rigid-body mass matrix	${}_T\mathbf{y}_v^i$	v th eigenvector restricted to the translational dof only of the i th modal basis
N	number of samples	${}_r\mathbf{y}_v^i$	v th eigenvector restricted to the sensor dof of the i th modal basis
\mathbf{S}^k	vector of optimal sensors dof at iteration k	\mathbf{R}	$n \times r$ rigid body modes matrix
\mathbf{Y}_i	$n \times m$ modal matrix corresponding to the i th sample	$\mathbf{\Lambda}$	diagonal spectral matrix
m	number of modes	$\ \mathbf{Y}_i\ _1$	vector of the sum of the columns in absolute value
		$\ \mathbf{y}_v^i\ _\infty$	maximal component in absolute value of the v th eigenvector of the i th modal basis

visibility of the variety of compromises at hand. However, the downside of a model-based analysis lies in the knowledge that the model behavior is only an approximation to the real system behavior. Hence the question of the honest designer: how sensitive is my measure of design success to uncertainties in my system representation?

The notion of uncertainty here is taken in a very general sense to include: epistemic uncertainties due to a lack of system knowledge, aleatory variability due to manufacturing processes and environmental conditions, the range of operational system configurations, and even uncertainties concerning the level of required performance. It is evident that if model-based analysis is to be used with any level of confidence then methodologies must be developed that no longer seek simply to optimize performance with respect to a given nominal model but rather attempt to satisfy an acceptable sub-optimal level of performance while remaining maximally robust to the system uncertainties.

In the context of the present article, we consider the specific design problem of planning vibration tests for a complex mechanical assembly. In the past two decades, a wide variety of deterministic model-based strategies have been developed to define an optimal configuration of sensors and actuators. In most cases, an optimal design is one which provides the best observability and distinguishability of the identified eigenmodes. For example, methodologies based on the Guyan reduction [1,2], the QR decomposition of the modal matrix [3], maximization of the determinant of the Fischer information matrix [4], entropy [5], minimum sensitivity to measurement noise [6] or to parameter variations [7]. In particular, this last reference defines optimality in terms of the confidence region resulting from the propagation of measurement errors to the identified model parameters.

In contrast to these strategies, we propose an approach for test planning which foregoes strict optimality and attempts merely to satisfy certain performance criteria while remaining maximally robust with respect to epistemic uncertainties in the nominal model. The latter may result from poorly estimated values for joint stiffnesses, geometric and material properties or even unmodelled behaviors such as nonlinear stiffness and damping in the structure. The foundations

of this robust-satisficing design approach has been developed in Refs. [8,9]. Moreover, we will focus on designing a robust test in view of identifying the modal parameters of the system from a set of measured frequency response functions resulting from base excitation tests. In this case, the test design problem reduces to choosing the number and the locations of the sensor dof. The performance of our test design will be evaluated using figures of merit based on the observability and distinguishability of the identified eigenmodes. However, other performance criteria could readily be included, such as maximizing the visibility of subdomains for error localization or maximizing the distinguishability of subdomains for model updating.

The proposed methodology comprises three phases. Firstly, a set of eigenbasis realizations is generated which is consistent with a predefined level of epistemic model uncertainty. Secondly, the global modes within each realization are selected based on the notion of effective masses [10,11]. Thirdly, the robust sensor design is determined by searching for the configuration which maximizes the worst-case distinguishability over the set of eigenbasis for a specified number of sensors. This last step is repeated for each additional sensor. The whole process is then restarted for the next level of epistemic model uncertainty.

The results of these calculations provide the basis for a test design decision-making tool allowing the decider to examine the trade-offs between marginal gain in performance for an additional sensor with respect to cost, as well as the degradation in performance for increasing levels of epistemic uncertainty. This approach is illustrated on an industrial model taken from the aerospace industry where the operational tests involve the application of base motion excitation. The latter are typically used in qualification tests in order to evaluate the system's dynamic response to launch or flight conditions.

2. Robust test design

We develop in this section the proposed robust test design methodology. Following a brief summary of info-gap decision theory, we will review the notion of effective mass which will allow us to select the global structural modes within a given frequency range. We will then define the figures of merit which will be used to measure the performance of a given test design and finally, the overall robust-satisficing optimization algorithm will be presented.

2.1. Info-gap robustness analysis

The objective of the proposed test planning methodology is to improve our model-based decision-making ability in the face of uncertainties. Among the more or less sophisticated quantifications of uncertainty, we choose here to base our approach on the info-gap decision theory [8,9] which is particularly relevant when the available knowledge about the uncertain model properties is severely limited.

Let $P(v)$ be the performance of a design (for example, eigenmode distinguishability) as a function of the design variables v (for example, the number and location of sensors). Then the notion of performance *satisficing* is expressed by

$$P(\hat{v}) \geq P_c$$

for a particular design \hat{v} and for some minimally acceptable performance P_c , where bigger is better. This approach can be contrasted to a design strategy based on optimizing (in this case, maximizing) the performance $P(v)$. In a robust-satisficing design strategy, we are prepared to sacrifice performance in order to maximize robustness to uncertainties.

Info-gap models quantify uncertainties as the size of the gap between what is known (nominal values of parameters $\tilde{\mathbf{u}}_i$) and what could be known (size of the domain of uncertainty). The gap is characterized by a scalar parameter α which represents the degree of uncertainty about the nominal values. In this example, we will use the following envelope bound info-gap model:

$$\mathcal{U}(\alpha, \tilde{\mathbf{u}}) = \left\{ \mathbf{u} : \left| \frac{\mathbf{u}_i - \tilde{\mathbf{u}}_i}{\tilde{\mathbf{u}}_i} \right| \leq \mathbf{w}_i \alpha \right\} \alpha \geq 0 \quad \text{for } i = 1, \dots, n, \quad (1)$$

where \mathbf{w} is a vector of weighting coefficients. The ensemble $\mathcal{U}(\alpha, \tilde{\mathbf{u}})$ thus represents a nested family of realizable parameter sets which is consistent with a given horizon of uncertainty defined by α .

The robust-satisficing solution for a test design based on c sensors is the configuration v which maximizes the info-gap robustness function $\hat{\alpha}(v, P_c)$

$$\hat{v}(P_c) = \arg \max_v \hat{\alpha}(v, P_c), \quad (2)$$

where $\hat{\alpha}(v, P_c)$ is defined by

$$\hat{\alpha}(v, P_c) = \max \left\{ \alpha : \min_{\mathbf{u} \in \mathcal{U}(\alpha, \tilde{\mathbf{u}})} P(v, \mathbf{u}) \geq P_c \right\}. \quad (3)$$

Remarks

- Eqs. (2) and (3) state that the robust-satisficing design is the one which maximizes the minimum level of performance for a given horizon of uncertainty.
- The critical performance P_c is not necessarily known a priori but will be chosen based on the results of the analysis where the trade-off between performance and the cost of allocating testing resources can be examined explicitly.
- Completely different solutions may arise for different horizons of uncertainty.

2.2. Mode selection

We are interested in designing a base excitation vibration test in the lower-frequency range. In the present context, the lower-frequency range refers to the frequency interval over which the eigenmodes are fairly well decoupled from one another, as opposed to the medium frequency range. The modal behavior of complex technological structures can still be quite complicated and it often proves to be important to automatically filter out local behaviors which are considered to be insignificant. Towards this end, we will use a global mode selection criterion based on the effective modal mass [11]. The global modes are those which have predominantly large reaction forces with respect to a rigid interface.

First, let \mathbf{R} be the rigid body matrix and \mathbf{Y} the fixed-base eigenvectors such that

$$\begin{aligned}\mathbf{R}^T \mathbf{K} \mathbf{R} &= 0; & \mathbf{R}^T \mathbf{M} \mathbf{R} &= \mathbf{M}_0, \\ \mathbf{Y}^T \mathbf{K} \mathbf{Y} &= \mathbf{\Lambda}; & \mathbf{Y}^T \mathbf{M} \mathbf{Y} &= \mathbf{I}_m,\end{aligned}$$

where \mathbf{M}_0 is the rigid body mass matrix. Let \mathbf{F} be the mass modal participation factor matrix defined by

$$\mathbf{F} = \mathbf{Y}^T \mathbf{M} \mathbf{R}.$$

The effective mass of mode i in the direction j due to an excitation k is then defined by

$$\mathbf{M}_{ijk}^{\text{eff}} = \frac{\mathbf{F}_{ij} \mathbf{F}_{ik}}{\mathbf{m}_{ii}}.$$

This quantity can be interpreted as a measure of the modal reactions due to a unit-base acceleration.

Remarks

- The sum of the effective masses over all modes is equal to the total mass \mathbf{M}_0

$$\sum_{i=1}^n \mathbf{M}_{ijk}^{\text{eff}} = \mathbf{M}_0 - \mathbf{M}_I,$$

where, generally, $\|\mathbf{M}_I\| \ll \|\mathbf{M}_0\|$ corresponds to the mass at the grounded interface dof.

It is not generally possible to compute all n normal modes. A residual mass matrix can be defined by

$$\mathbf{M}_{mjk}^{\text{res}} = \mathbf{M}_0 - \sum_{i=1}^m \mathbf{M}_{ijk}^{\text{eff}}.$$

- An eigenvector will be considered to be global if at least one of the values of the effective masses along the 3 translational and the 3 rotational directions is greater than 1% to 10% of the rigid body mass.

2.3. Observability

We will now consider two figures of merit that will provide a measure for the performance of a given test design, namely the *observability* and the *distinguishability* of the identified eigenmodes. First, let us consider the first figure of merit—observability. Qualitatively, an eigenmode is considered to be observable if at least one sensor shows a significant level of response with respect to the maximum response level for that mode.

Let ${}_T \mathbf{y}_v^i$ and ${}_r \mathbf{y}_v^i$ be the v th eigenvectors of the i th basis restricted to the translational dof and the retained sensors dof, respectively. The observability κ_v^i is measured a posteriori using a criterion based on a ratio of the maximal component of each eigenvector at the sensors dof and the

maximal component of each eigenvector at all candidate dof

$$\kappa_v^i = \frac{\|r\mathbf{y}_v^i\|_\infty}{\|T\mathbf{y}_v^i\|_\infty}. \quad (4)$$

Remarks

- The observability criterion lies on the interval $[0; 1]$.
- A small value of κ_v^i indicates that maximal component of the v th eigenvector among all sensors dof is small compared with the maximal component of the v th eigenvector among all translational dof, then mode v of the i th basis is not observable whereas a value of κ_v^i near 1 indicates that the mode is observable vis-a-vis the sensor locations.

2.4. Distinguishability

The second figure of merit is based on the *distinguishability* of the eigenmodes corresponding to a given eigenbasis realization. Qualitatively, a set of eigenmodes is considered to be distinguishable when no single eigenvector can be written as a linear combination of the remaining eigenvectors in the basis. The distinguishability of an eigenbasis will be quantified here by the condition number where distinguishability improves with decreasing condition number.

Let \mathbf{Y}_i be the modal matrix for the i th sample, \mathbf{S}^{k-1} the vector of optimal sensors dof defined at iteration $k-1$, \mathbf{D}_j the j th element of a set of candidate dof and $\mathbf{Y}_i(\mathbf{S}^{k-1}, \mathbf{D}_j)$ the modal matrix \mathbf{Y}_i restricted to the set of dof defined by \mathbf{S}^{k-1} and \mathbf{D}_j . At the k th iteration, the optimal location of the k th sensor is defined by

$$\mathbf{S}^k = \left\{ \{\mathbf{S}^{k-1}, \mathbf{D}_j\} : \min_{\mathbf{D}_j} \left(\max_{\mathbf{Y}_i} (\text{cond}(\mathbf{Y}_i(\mathbf{S}^{k-1}, \mathbf{D}_j))) \right) \right\}. \quad (5)$$

To start the procedure, the first sensor location is chosen by finding the candidate dof which maximizes the sum of the columns of the modal matrix

$$\mathbf{S}^1 = \left\{ \mathbf{D}_j : \max_{\mathbf{D}_j} \left(\min_{\mathbf{Y}_i} (\|\mathbf{Y}_i(\mathbf{D}_j)\|_1) \right) \right\}. \quad (6)$$

While other selection criteria for the first sensor are possible, Eq. (6) generally leads to reasonable observabilities for a large number of modes when such a dof exists.

2.5. Solution algorithm

The solution of the optimization problem defined by Eq. (2) is by no means easy. Firstly, the search for a strictly optimal location of n^s sensors given n candidate values rapidly becomes intractable. Secondly, searching for the worst-case performance over the bounded set defined by Eq. (1) for a non-convex solution space is also impracticable. We are thus obliged to admit that it is unrealistic to search for a strictly rigorous solution to the posed optimization problem. The

following two compromises are thus invoked in order to obtain pertinent solutions in a reasonable time:

- We will replace the strictly combinatorial problem of searching for the best c sensors, $c = 1$ to n^s , given n candidate values by a sub-optimal solution whereby the sensors are added one by one while retaining the sensor locations selected at the previous step.
- We will generate a set of N eigenbasis realizations which are consistent with Eq. (1). These realizations will then represent the model space over which the locations of n^s sensors will be sought so as to maximize the worst-case performance.

The robust test planning algorithm is then implemented as follows:

1. Choose a value α defining a horizon of uncertainty.
2. Generate a set of N eigenbasis realizations using a latin hypercube sampling.
3. Filter out the local modal behaviors for each eigenbasis using the effective mass criteria.
4. For $i = 1$ to n^s , determine the sensor test design that maximizes the minimum distinguishability over the set of eigenbasis realizations. Do this in a sub-optimal manner by retaining at the step i the $i - 1$ previously defined sensor positions.
5. Increment α and go to step 1, otherwise stop.

3. Industrial application

3.1. Finite element (FE) model description

The proposed robust test planning procedure is illustrated on the application PASTEC shown in Fig. 1. PASTEC is a technological demonstration passenger developed by the CNES and carried by the SPOT 4 satellite. It includes seven technology demonstration experiments to improve our knowledge of the space environment and the phenomena affecting the behavior of orbiting spacecraft. The PASTEC structure is composed of a primary truss of 12 rods with a tubular section, a sandwich baseplate with aluminium skins and honeycomb core supporting 10 pieces of equipment and a secondary truss supporting the Multi-Layer Insulation and the radiator.

The FE model contains 2537 nodes and 2830 elements. The sensor candidate dof set includes all translational dof of beams elements and the dof along the x -axis for one-fourth of the nodes belonging to shell elements. The three directions, along the three axis x , y and z , are considered in the present example for base excitation.

The first eigenfrequencies of the nominal model and their associated maximal effective masses are shown in Table 1. In the case of the nominal model and for a threshold of 1% of the rigid body mass, only the modes 1, 9, 10, 11, 14, 15, 19, 20 and 21 are selected for the test planning procedure. The mode shapes corresponding to mode 10, 11, 15 and 20 are shown in Figs. 2–5. However, the set of global modes will generally be different for each eigenbasis realization.

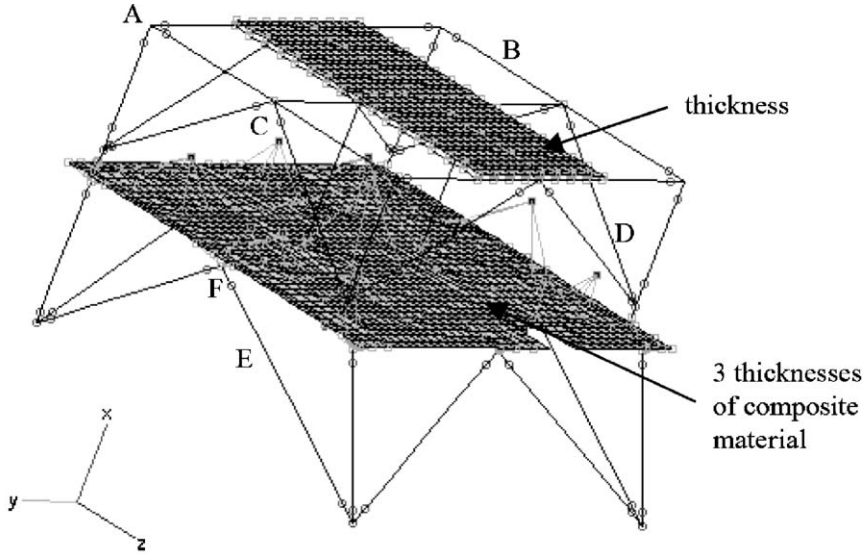


Fig. 1. PASTEC structure and uncertain parameters.

3.2. Results

The 16 uncertain parameters u_i considered here are shown in Fig. 1. Points A to D represent the bars of secondary truss while points E and F represents bars of the primary structure. Bars A and F are used to model the interfaces between the horizontal, vertical, and diagonal structural elements. The 16 uncertain parameters are the quadratic moments of inertia of all the bars, the thickness of the radiator and the 3 thicknesses of the skins and the baseplate core. Their nominal values are shown in Table 2. Note that the quadratic moments of inertia are considered uncertain for all bars having the same role in the four faces of the structure.

The observability and distinguishability criteria is evaluated for three values of α namely (0.1, 0.2, 0.3) which correspond to three levels of uncertainty for all parameters of $\pm 10\%$, $\pm 20\%$ and $\pm 30\%$ (all weighting coefficients $w_i = 1$). For each value of α , a sample of $N = 75$ eigenbasis realizations are generated using a Latin hypercube algorithm [12]. A global mode selection is performed based on effective masses with a threshold ratio between the effective mass values and the structural mass equal to 1%.

3.2.1. Distinguishability

For each value of α , sensor locations are determined using Eq. (5). The results for the nominal model and for the three values of α are shown in Fig. 6 which illustrates the trade-off between allocated resources (number of sensors) and performance (level of distinguishability expressed by the condition number) as well as the impact of increasing model uncertainty. For example, if we consider that uncertainties of $\alpha = 0.2$ are consistent with our available knowledge of the FE model, the best distinguishability is obtained for 25 sensors while if we consider an uncertainty

Table 1
Eigenfrequencies and maximum of effective mass of the nominal model

No.	Eigenfrequency (Hz)	$\max(M_{\text{eff}})$
1	76.29	1.45
2	77.44	0.30
3	77.78	0.003
4	78.77	0.013
5	79.23	0.003
6	79.69	0.11
7	79.84	0.44
8	79.85	0.003
9	87.56	1.99
10	113.9	27.7
11	117.5	1.35
12	117.6	0.015
13	117.7	0.0002
14	117.9	3.80
15	124.4	18.23
16	131.9	0.07
17	132.4	0.27
18	134.8	0.39
19	136.6	11.7
20	147.7	37.2
21	149.7	9.6

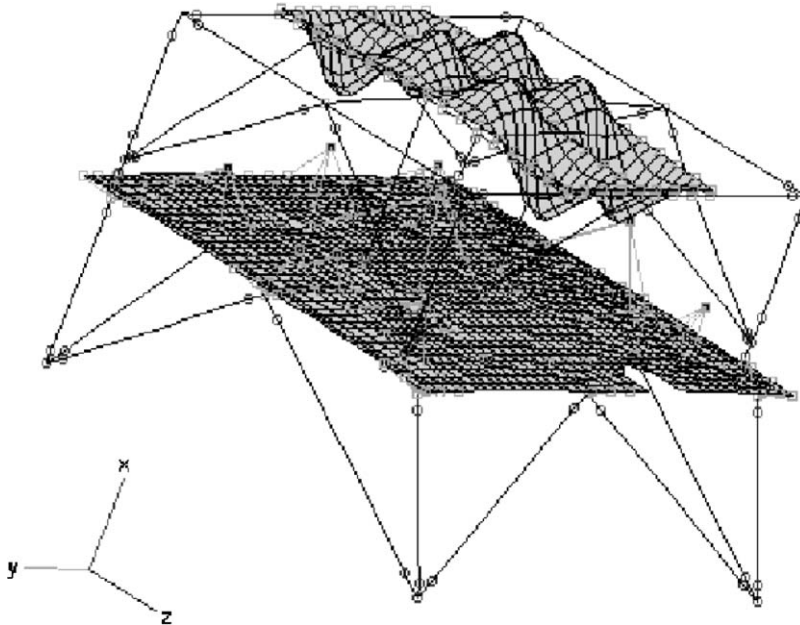


Fig. 2. PASTEC mode 10.

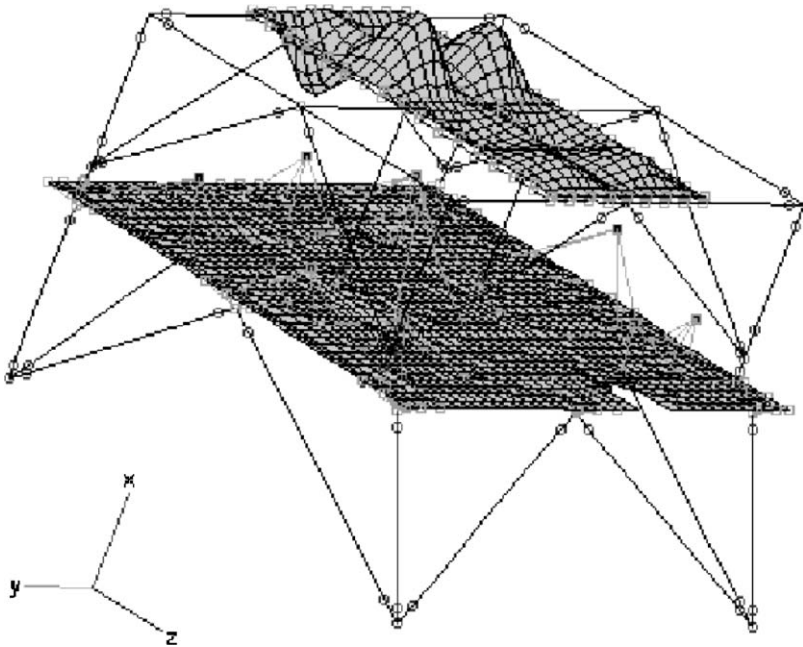


Fig. 3. PASTEC mode 11.

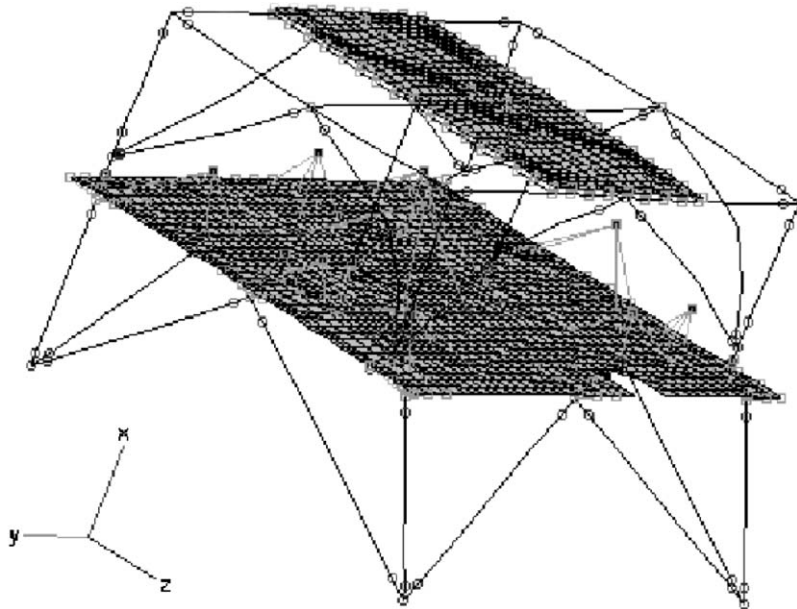


Fig. 4. PASTEC mode 15.

level $\alpha = 0.1$, only 13 sensors are needed to obtain the same level of distinguishability. This kind of information allows us to evaluate the sensitivity to uncertainty as well as the marginal gain resulting from the addition of new sensor.

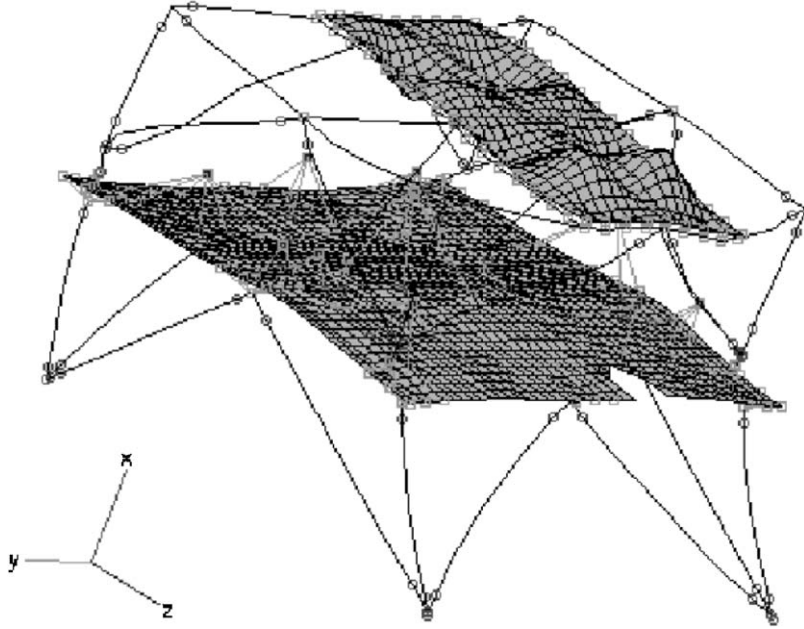


Fig. 5. PASTE mode 20.

Table 2
Uncertain parameters

Parameter	Nominal value
First quadratic moment of inertia of bars A	$1.143 \times 10^{-9} \text{ m}^4$
Second quadratic moment of inertia of bars A	$1.46 \times 10^{-10} \text{ m}^4$
First quadratic moment of inertia of bars B	$1.959 \times 10^{-9} \text{ m}^4$
Second quadratic moment of inertia of bars B	$1.959 \times 10^{-9} \text{ m}^4$
First quadratic moment of inertia of bars C	$1.143 \times 10^{-9} \text{ m}^4$
Second quadratic moment of inertia of bars C	$1.46 \times 10^{-10} \text{ m}^4$
First quadratic moment of inertia of bars D	$1.754 \times 10^{-9} \text{ m}^4$
Second quadratic moment of inertia of bars D	$1.3 \times 10^{-10} \text{ m}^4$
First quadratic moment of inertia of bars E	$2.13 \times 10^{-8} \text{ m}^4$
Second quadratic moment of inertia of bars E	$2.13 \times 10^{-8} \text{ m}^4$
First quadratic moment of inertia of bars F	$1.143 \times 10^{-9} \text{ m}^4$
Second quadratic moment of inertia of bars F	$1.46 \times 10^{-10} \text{ m}^4$
Radiator thickness	0.0006 m
Baseplate skins thicknesses	0.0008 m
Baseplate core thickness	0.0434 m

For benchmark purposes, the maximum condition number (worst-case distinguishability) for all eigenbasis realizations restricted to their translation dof is calculated to be 8.26 and is shown as a dashed line in Fig. 6. The diminution of the condition number begins when the number of

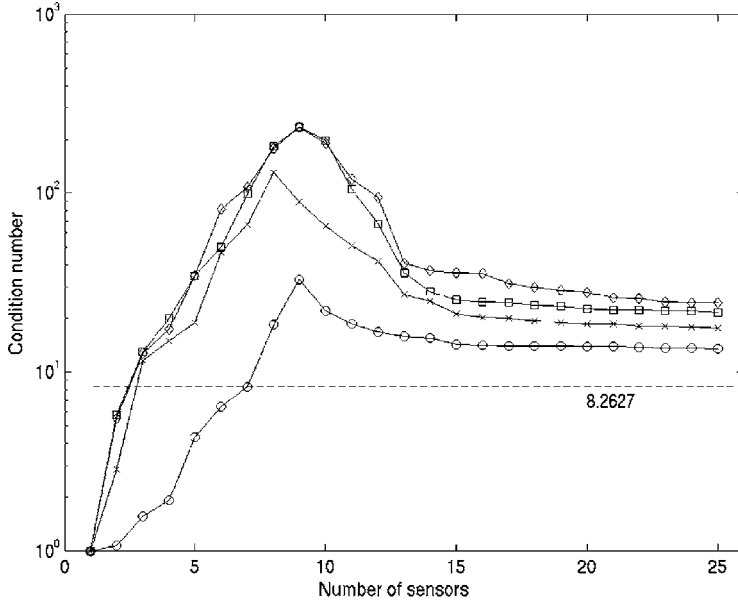


Fig. 6. Evolution of the robust condition number: ○ nominal; × $\alpha = 0.1$; □ $\alpha = 0.2$; ◇ $\alpha = 0.3$; - - max (cond(Y_i)).

sensors is greater than the maximal number of selected modes among the basis Y_i for each value of α .

The robust sensor design is shown in Fig. 7 for the uncertainty level $\alpha = 0.2$ and a number of sensors equal to 25. Note that 3 sensors are not visible due to the orientation of the 3D visualization.

The evolution of the robust condition number as a function of the number of sensors and their corresponding observation direction is reported in Table 4.

We present in Table 3 the results obtained by applying the optimal sensor design based on the deterministic nominal model to the eigenbasis realizations Y_i ($i = 1-75$), for each level of uncertainty α . The best and the worst distinguishabilities, corresponding to the lowest and highest condition numbers, can be compared to the robust distinguishability obtained from Eq. (5) where the results have been computed for 25 sensor dof. We note the following tendencies:

- The optimal deterministic design can lead to both very good and very poor distinguishabilities over the space of model uncertainties, as seen in the first two rows in Table 3.
- The robust design sacrifices optimal values of distinguishability while insuring worst-case values which are much better than those of the deterministic design, as seen in the third row in Table 3.

3.2.2. Observability

The observability is computed a posteriori using Eq. (4) for the nominal model. Fig. 8 illustrates the typical evolution of the observability for a few modes and we note that the first sensor allows us to observe mode number 20. This behavior is typical for about all modes, and in particular

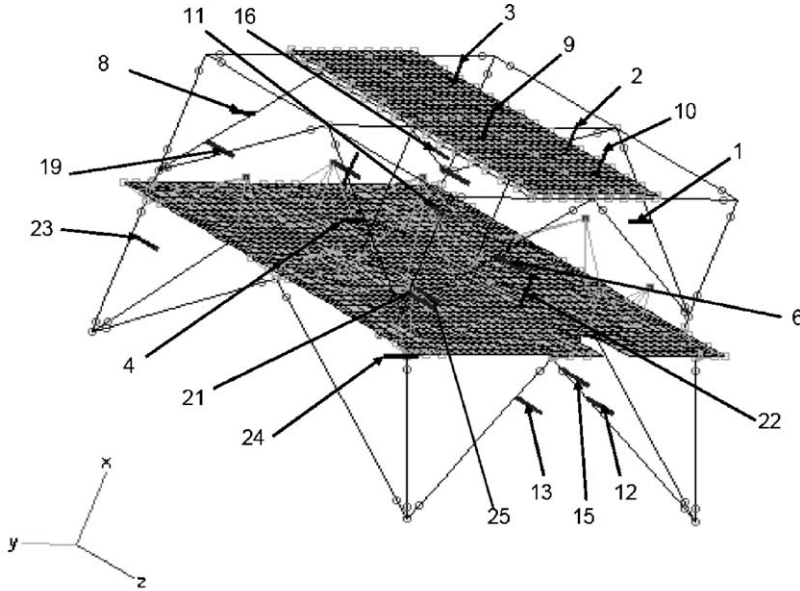


Fig. 7. Robust sensor location for $\alpha = 0.2$.

Table 3
Distinguishability for deterministic and robust designs

	Nominal	$\alpha = 0.1$	$\alpha = 0.2$	$\alpha = 0.3$
Best condition number	13.55	7.23	6.33	6.02
Worst condition number	13.55	45.44	86.36	238.9
Robust condition number	13.55	17.53	21.65	24.36

mode 15, which have large effective masses along the direction of the first sensor (y) shown in Fig. 7. The modes 10 and 11 have large effective masses along the x -direction. The first sensor along the x -direction is added to the test design in second place. We note that the observability is not as large as expected. This is due to the fact that the first sensor in the x -direction is near a nodal line of the modes 10 and 11. By adding 3 more sensors along the x -direction, modes 10 and 11 become observable once the total number of sensors exceeds 10 as shown in Table 4.

4. Conclusion

A method for the robust design of base excitation vibration tests is proposed based on a info-gap robust-satisficing design approach. The performance of the test design is measured primarily by the distinguishability of the observable eigenbasis. Optimal performance based on a deterministic nominal model is sacrificed in order to obtain a solution which satisfies a minimum

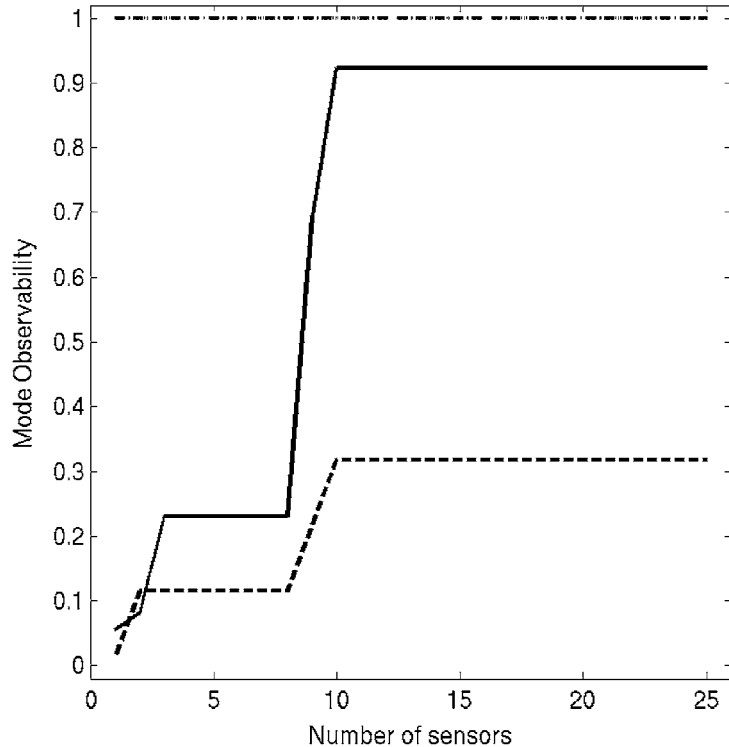


Fig. 8. Observability wrt number of sensors: — mode 10; -- mode 11; - · - mode 15; · · · mode 20.

Table 4
Evolution of condition number for $\alpha = 0.2$

Sensor number	1	2	3	4	5	6	7	8	9	10
Condition number	1	1	1.02	1.31	1.96	2.07	6.32	6.73	11.2	14.2
Direction	2	1	1	2	2	3	3	2	1	1
Sensor number	11	12	13	14	15	16	17	18	19	20
Condition number	34.8	25.5	21.2	18.7	17	15.7	14.6	13.8	13.5	13.2
Direction	3	3	3	3	3	3	1	3	1	3
Sensor number	21	22	23	24	25					
Condition number	13.2	12.9	12.6	12.6	12.5					
Direction	3	1	3	2	3					

level of distinguishability while maximizing robustness to uncertainties in the model. The latter are due not only to tolerances in material properties and manufacturing processes, but also to the use of uncertain modelling rules (simplified connectivities, homogenized properties, poorly estimated stiffness and damping laws, etc.). Since the test planning is prepared based on a non-validated model, we have assumed that very limited information is available concerning the details of the

uncertainties affecting the model variables and this has lead us to adopt an uncertainty model which is consistent with our available knowledge, namely an info-gap uncertainty approach.

The proposed methodology is applied to a small industrial example taken from the aerospace field in order to illustrate the significant impact that model variability can have on the chosen optimality criteria and to highlight the importance of taking this variability into account in the test planning process. Future work will focus on introducing other types of optimality criteria into the design objectives, for example, parameter visibility and distinguishability for model error localization purposes, and mode excitability for input design. Moreover, the impact of aleatory errors in the eigenvector measurements might also be introduced in order to complete the representation of uncertainty in the test planning process.

References

- [1] D.C. Kammer, C.C. Falnigan, W. Dreyer, A super-element approach to test-analysis model development, *Proceedings of the Fourth International Modal Analysis Conference*, 1986, pp. 663–673.
- [2] G. Lallement, A. Ramanitraja, S. Cogan, Optimal sensor deployment: application to model updating, *Journal of Vibration and Control* 4 (1998) 29–46.
- [3] C. Schedlinski, M. Link, An approach to optimal pick-up and exciter placement, *Proceedings of IMAC XIV*, 1996, pp. 376–382.
- [4] A. Linderholt, T. Abrahamsson, Parameter identifiability in finite element model error localisation, *Mechanical System and Signal Processing* 17 (2003) 579–588.
- [5] C. Papadimitriou, J.L. Beck, S.K. Au, Entropy-based optimal sensor location for structural model updating, *Journal of Vibration and Control* 6 (2000) 781–800.
- [6] T. Potshiri, K.D. Hjelmstad, Strategy for finding a near optimal measurement set for parameter estimation from modal response, *Journal of Sound and Vibration* 257 (2002) 89–106.
- [7] T. Kurita, K. Matsui, Confidence region of identified parameters and optimal sensor locations based on sensitivity analysis, *Structural Engineering and Mechanics* 13 (2002) 117–134.
- [8] Y. Ben-Haim, *Robust Reliability in the Mechanical Sciences*, Springer, Berlin, 1996.
- [9] Y. Ben-Haim, *Information-gap Decision Theory: Decisions Under Severe Uncertainty*, Academic Press, San Diego, 2001.
- [10] U. Füllekrug, Determination of effective-masses and modal masses from base-driven tests, *Proceedings of the 14th International Modal Analysis Conference*, Dearborn, Michigan, 12–15 February 1996.
- [11] R. Sedeghati, Y. Soucy, N. Etienne, Efficient estimation of effective mass for complex structures under base excitations, *Canadian Aeronautics and Space Journal* 49 (3) (2003).
- [12] D.E. Huntington, C.S. Lyrintzis, Improvements to and limitations of Latin hypercube sampling, *Probabilistic Engineering Mechanics* 13 (1998) 245–253.